ResearchGate

See discussions, stats, and author profiles for this publication at: https://www.researchgate.net/publication/308044923

Synthesis of PVDF/CNT and their functionalized composites for studying their electrical properties to analyze their applicability in actuation & sensing

Article *in* Colloids and Surfaces A Physicochemical and Engineering Aspects · September 2016

DOI: 10.1016/j.colsurfa.2016.09.007

CITATIONS
69

READS
1,774

5 authors, including:

Soumya ranjan Mishra
Central Electrochemical Research Institute

12 PUBLICATIONS **2,503** CITATIONS

SEE PROFILE

Kumaran K T

4 PUBLICATIONS **284** CITATIONS

SEE PROFILE

All content following this page was uploaded by Soumya ranjan Mishra on 28 December 2018.

The user has requested enhancement of the downloaded file.

MRD EX. 2014
LGES v MRD
IPR2024-01013

Colloids and Surfaces A: Physicochem. Eng. Aspects 509 (2016) 684–696

Contents lists available at ScienceDirect

Colloids and Surfaces A: Physicochemical and Engineering Aspects

journal homepage: www.elsevier.com/locate/colsurfa

Synthesis of PVDF/CNT and their functionalized composites for studying their electrical properties to analyze their applicability in actuation & sensing

Soumyaranjan Mishra [a], K.T. Kumaran [a], R. Sivakumaran [b], S. Paul Pandian [b,*], Subrata Kundu [a,c,**]

[a] Electrochemical Materials Science (ECMS) Division, CSIR-CECRI, Karaikudi, India
[b] Advanced Inertial System, IISU-ISRO, Trivandrum, Kerala, India
[c] Department of Materials Science and Mechanical Engineering, Texas A&M University, College Station, TX, TX-77843, USA

HIGHLIGHTS

- We have proposed an easy way to synthesize carbonic and sulphonic acid functionalized CNT-PVDF nanocomposites and successfully used as nano-fillers for piezo-polymers.
- Based on thermal analysis and SEM results, we can claim that our fabricated materials can remain stable up to 490 °C.
- The synthesized nanocomposites are analysed by various electrochemical studies and successfully applied as potential materials for 'Actuators' or 'piezoelectric sensors'.
- Electrochemical study reveals that on adding COOH functionalization to PVDF + CNT, it enhanced the conductivity, electro-resistive behaviour but decreasing the capacitance although SO_3H functionalised CNT-PVDF composite suffers from uneven sulphur doping.
- Finally, our present study reveals that COOH functionalized CNTs are better nanofillers for PVDF than only CNTs but SO_3H functionalized CNTs are not, for the application in actuation or sensing.

GRAPHICAL ABSTRACT

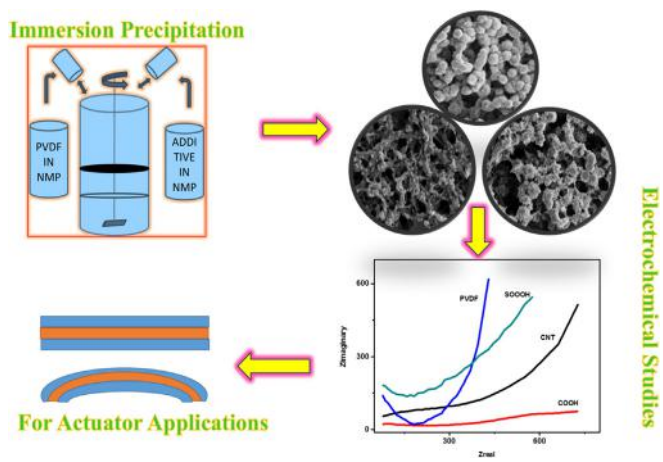

ARTICLE INFO

Article history:
Received 23 June 2016
Received in revised form 31 August 2016
Accepted 2 September 2016
Available online 11 September 2016

ABSTRACT

The actuation properties of piezo-electric polyvinyl di fluoride (PVDF) can be improved by mixing electro-resistive carbon nano tubes (CNT's) and various mechanisms have been highlighted recently. Herewith, we proposed a simple route for the synthesis of PVDF/CNT composite by mixing a proper concentration of

* Corresponding author.
** Corresponding author at: Electrochemical Materials Science (ECMS) Division, CSIR-CECRI, Karaikudi, India.
E-mail addresses: s_paul_pandian@vssc.gov.in (S.P. Pandian), skundu@cecri.res.in, kundu.subrata@gmail.com (S. Kundu).

http://dx.doi.org/10.1016/j.colsurfa.2016.09.007
0927-7757/© 2016 Elsevier B.V. All rights reserved.

Keywords:
PVDF
NMP
CNT
Composites and actuator

PVDF with CNT in N-Methyl-2-pyrrolidone (NMP) by using solution phase co-precipitation techniques. We observed that at a certain concentration ratio of PVDF and CNT, it formed well crystalline morphology with specific structures. After optimizing their concentrations, we mixed carbonic and sulphonic acid functionalized CNT with PVDF at a certain ratio and prepared the acid functionalized PVDF/CNT composites. The composite materials were characterized by various spectroscopic and microscopic techniques such as XRD, FTIR, thermal and FE-SEM analyses. From the FE-SEM analysis, the sheikh kabab morphology was observed in PVDF while more pronounced and oriented structure was found in case of CNT as well as their carbonic acid functionalized product. As an application, the synthesized materials are studied for actuation purposes by investigating their properties using cyclic voltammetry (CV) and electrochemical impedance spectroscopy (EIS) analysis. It was observed that the actuation properties of PVDF was enhanced while mixed with CNT and carbonic acid functionalized CNT although it remained unchanged in case of sulfonic acid functionalized CNT. In case of PVDF and carbonic acid functionalized CNT, a higher saturation current of 2.7 mA was observed while for bare PVDF in NMP, a reduced value of 0.0087 mA was observed. The present synthesis route and the application process is simple, less time consuming and could be extended for the fabrication of other composite materials for their potential application as actuator and in other technologically important energy related fields.

© 2016 Elsevier B.V. All rights reserved.

1. Introduction

In the field of sensing and actuation, piezoelectric materials are one of the most commonly applied assemblage of materials today. Their basic principle is the effect of generating electricity based on application of mechanical stress. The charge hence generated is a direct function of piezoelectric strain constant and applied force. Likewise, on applying an electric excitation, they produce mechanical deformation, called reverse piezoelectric affect. This reversible nature was thermodynamically established in 1881 [1]. The first known instance of discovery of this phenomenon goes back to 1880 when Dr. Pierre and his elder brother Jacques Curie prepared special crystals like quartz, topaz and Rochelle salt and demonstrated that applying a sufficient mechanical stress, they could generate a surface charge [2,3]. Apart from that, they also compiled proof of the linear and reversible nature of Piezoelectricity. Piezoelectric materials can be used as ultrasonic waves producers and detectors, sensing elements, actuators, accelerometers and numerable other applications. Among the various forms of piezoelectric materials, one of the most researched material is piezo-films that can be applied as actuators. They are used as transducer since they do possess an incredible array of properties viz., are extremely light weight, have wide frequency range (0.001 Hz to 10^9 Hz), vast dynamic range (10^{-8}–10^6 psi) and low acoustic impedance that resembles that of water, human tissue and adhesive systems [1]. Besides, they also possess high elastic compliance, high voltage output, high dielectric strength, resist moisture (<0.02% moisture absorption), intense ultraviolet and nuclear radiation and moreover they can be fabricated into unusual designs.

After 50 years of the discovery of piezoelectric polymer, now it has emerged as a highly commercialised technology [4]. In actuation, the most commonly used fluoropolymer, Polyvinylidene fluoride (PVDF) was actually found to possess such high piezoactivity by Kawai [2]. Till date, PVDF and its copolymers are much more piezo active then than other polymers. Hence, PVDF, especially in its electroactive β-phase [5], is the most investigated polymeric piezo material. Poling is done to convert α-PVDF to β-PVDF, which is the more polar form [6,7] . Its high chemical and thermal tolerance only add to its attractiveness. One of the most important achievements in recent times involve addition of attractive electrical properties to the mechanical response of polymeric materials by means of suitable nano-fillers [8–10]. About a decade and half ago, the ability of structural materials to sense their own strain has been reported in carbon nanotubes (CNTs) polymer–matrix composites [11]. One such novel nano-composite comprises CNT-Polymer system which utilises the exquisite combination of high electrical property of CNT and excellent mechanical property of Polymers. Both single walled carbon nanotubes (SWCNT) and multi walled carbon nanotubes (MWCNT) have been applied as accurate strain nanoscale sensors based on correlation between their reversible mechanical deformation and electrical resistance [9]. Moreover, further improvement has been demonstrated through direct dispersion of individual CNTs in a polymer and it has been shown that the electrical resistance of the resulting composite changes with strain [12]. The piezo-resistive properties of CNT nanocomposites are controlled by interactions between the CNT networks as opposed to the intrinsic piezoresistive effect, which affects the electrical properties of individual CNTs with change in applied stress or strain [9]. By addition of carbon nano-fillers, dielectric polymer matrix can be made electrically conductive and the corresponding changes in electric resistance of materials under applied stress and strain becomes more prominent. In this way, strain sensing is possible with piezoresistive materials and more precisely, polymeric nanocomposites materials are the best suited materials for this types of application as they can be designed for required stress or strain.

Now a days, a high level of investigation has been attempted to increase the dispersion of CNTs in various matrix materials through pre-treatment functionalization methods and mixing procedures to obtain enhanced properties of the composite materials [13]. The functionalization of CNT comes at the expense of carbon–carbon bond cleavage and reduction in the p-bonding network which may lead to a loss of electrical conductivity [14]. CNT dispersion can also be done by utilizing small molecule and oligomeric additives which have high affinity towards CNT surface and can wrap around the tubes to reduce aggregation via noncovalent functionalization. O'Brian et al. explored the possibilities of CNT-filled polymers for electromagnetic coating technologies and used PVDF as the matrix material in their study due to the excellent coating properties [14]. Sun et al. [15], reported on a model with experimental support to understand the interaction of mixed fill systems composed of carbon black or graphite with MWCNT. Spitalksy et al. [16] demonstrated the effects of various oxidative treatments on MWCNTs in epoxy composites. They found that stronger oxidative treatments decrease electrical conductivity due to damage to the MWCNT outer wall and disruption of the p-bonding network. Jung et al. [17] have recently reported that improved dispersion occurs as a result of vacuum ultraviolet oxidative treatment of MWCNT provides enhanced thermal, electrical, and mechanical properties. Yu et al. prepared two PVDF/CNT composites by solution sonication and

mechanical mixture approaches and observed that α-phase coexists with β-phase in the composite prepared by sonication while no β-phase was observed in the composite prepared from the mechanical mixture route [18]. Li et al. reported that SWNTs film can be used as strain sensor at the macro scale due to the dependence of the electrical properties of the SWNTs film on mechanical deformation on nanoscale [19]. Paulson et al. studied the response of the MWCNT to mechanical strain applied with atomic force microscope [20]. The critical content of CNTs that characterizes a drastic increase in conductivity is commonly termed as the electrical percolation threshold (EPT) [21]. Recently, Zeng et al. have shown a threshold value of 3.2 wt% of MWNTs for percolation to occur in epoxy/CNT composite based on conductivity-concentration plot and using Monte-Car lo simulations [22]. Moreover, inclusion of CNT leads to lower percolation threshold as compared to other conductive fillers. Hence, to effectively utilise CNT as fillers in polymers, one needs to ensure their homogenous dispersion throughout the matrix without destroying their integrity [23]. There are very few reports on electrical properties of PVDF/CNT using carbonic acid functionalised CNT's, but to the best of our knowledge, the electric properties of sulphonic acid functionalised CNT's and PVDF composites are yet to be done. So we opt for the electrochemical study with the carbonic acid and sulfonic acid functionalized CNT/PVDF composites.

Based on our knowledge about PVDF and CNT nanocomposites, in the present paper, we have electrochemically analysed the piezo-resistive response of PVDF/CNT composite and that of their functionalized CNT composites (via carbonic and sulfonic acid). Following which, we have compared the response of these PVDF/CNT functionalized samples with that of PVDF and PVDF/CNT composite. The synthesized materials and their composites has been tested and compared for the application as actuators or piezoelectric sensors. For the synthesis, we dissolved the PVDF in NMP base (co-precipitation method) [10] and dispersed the CNT and the functionalised CNTs over the polymer matrix to prepare the sample which was followed by drying for 70 to 80 h in ambient conditions. Finally, the samples are hot-pressed to get thin films of uniform thickness of 200–300 μm. The synthesized composite materials were characterized by different spectroscopic and microscopic techniques. Herein through electrochemical analysis, we intend to prove that COOH functionalised CNT is better nanofillers than CNTs and investigate if SO_3H functionalised CNTs are equally promising. For the application as actuators or piezoelectric sensors, the properties of synthesized materials are studied using cyclic voltammetry (CV) and electrochemical impedance spectroscopy (EIS) analysis. It was observed that the actuation properties of PVDF was enhanced while mixed with CNT and carbonic acid functionalized CNT, although it remained unchanged in case of sulfonic acid functionalized CNT. The present synthesis and the application process is simple, less time consuming and could be extended for the fabrication of other composite materials for various energy and sensing related fields within a shorter time scale.

2. Experimental

2.1. Chemicals and instruments

α-phase polyvinylidene fluoride (PVDF, $(C_2H_2F_2)x$) in the form of white nano powder was purchased from Sigma-Aldrich having an average molecular weight of 5,34,000 (by GC). *N*-Methyl-2-pyrrolidone [NMP (C_5H_9NO)] was also obtained from Sigma-Aldrich and used as solvent for PVDF. It had a molar mass of 99.13 g/mol, density of 1.028 g/cm^3 and boiling point of 202 to 204 °C. The MWCNT and functionalised CNT's (Carbonic acid and Sulphonic acid functionalised) with a given specification of 10–50 nm were procured from Thomas scientific.

The synthesized samples were characterized using Fourier Transform Infrared Spectroscopy (FT-IR) using Jasco FT-IR 6600 and Raman Spectroscopy (Horiba Xplora ™ plus) using 532 nm LASER in the wavenumber range of 4000–400 cm^{-1}. The thermal gravimetric and differential thermal analysis (TGA/DTA) was done by providing a ramp input of 10–900 °C using 2960 SDT V3.0F set up. X-ray diffraction (XRD) analysis was done using D8 Discover Bruker X-ray diffractometer. The morphological changes of the above samples were investigated using field emission scanning electron microscopy (FE-SEM) having model number Sigma 500 of Carl Zeiss. Energy dispersive X-ray spectroscopy (EDS) analysis was done using Sigma 500 of Carl Zeiss. We have also analysed the electrochemical properties of our samples via electrochemical Impedance Spectroscopy (EIS) and Cyclic Voltammetry (CV) studies using Versa PARSTAT apparatus.

2.2. Preparation of PVDF/CNT composite and functionalize CNT composites

The PVDF/CNT composite and functionalized CNT/PVDF composites are prepared as follows. A definite amount of PVDF is weighed out into an empty beaker. NMP is then weighed and poured over PVDF till it's soluble. Proper mechanical agitation is then ensured for prolonged time (about 2 h) followed by ultrasonication for an hour to get homogenous solution. The solution is then poured as thin films over glass and dried in air. Then hot pressing is done at 80 °C for 5 min and the sheets hence obtained of desired thickness are cut into uniform size and shape. After that cooling and drying is carried out in ambient conditions to get smooth and well-desiccated films. Besides PVDF, mixtures of PVDF with multi-walled Carbon Nano-tubes (CNT) at various concentrations were prepared and above procedures were followed. A separately prepared well dispersed CNT solution in NMP was added to PVDF solution as prepared above (by mechanical agitation) and sonicated. For a typical reaction, various amounts such as 0.1, 0.2, 0.3, 0.4 and 0.5 g of CNT per 2 g of PVDF were prepared with a motive to optimise the concentrations. After that CNT functionalised with carbonic acid and sulphonic acid was mixed with PVDF and films were prepared at varying concentrations of 0.2 and 0.3 g per 2 g PVDF. The CNT and functionalised CNT's with a given specification of 10–50 nm were procured from Thomas scientific. For hot pressing, maximum temperature of 80 °C was used to preserve PVDF in the piezo-electric β stage. After preparing the films, they are cut into regular shapes and sizes for analysis as discussed in schematics in Scheme 1. The films were actually pressed between two steel crucibles held intact by a Teflon cylindrical cover and brass plates at two ends [24]. At these ends we have outlets for power connections as shown in Scheme 2. From one port we make connections for working electrode and from other port we make connections for reference and counter electrodes for electrochemical studies. As discussed before, electrical percolation threshold is directly related to good conductivity of samples [21]. So, at first using LCR meter we made conductivity studies for PVDF/CNT samples to optimise the concentration of CNT. Since, CNT with composition as in sample 4, shows better electrical conductivity (increasing concentration of CNT above this has negligible effect on DC conductivity), the other samples of same compositions were chosen. Four different samples (numbered 1, 4, 9 and 10 from table) have been analysed for CV and EIS respectively. For CV, a voltage ranging from 0 to 1 V has been applied at a constant scan rate of 0.05 V/s with the area of working electrode being 1 cm^2. Similarly, for EIS, amplitude of 10 mV RMS is fixed with a scan rate of 0.005 V/s and a frequency ranges starting from 10 Hz to 2 MHz to get optimum readings. The precise quantities of various chemicals taken are shown in Table 1. The prepared

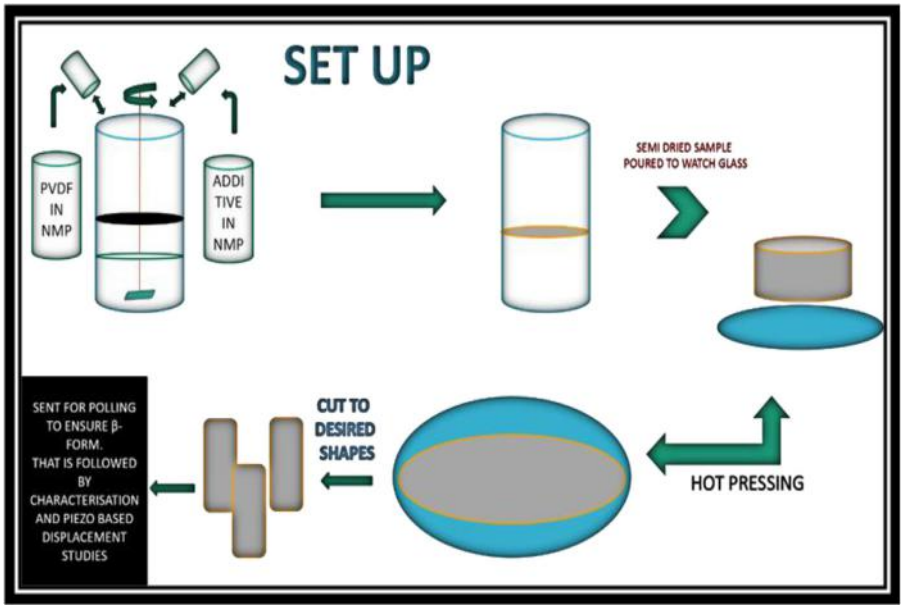

Scheme 1. Schematics of our process.

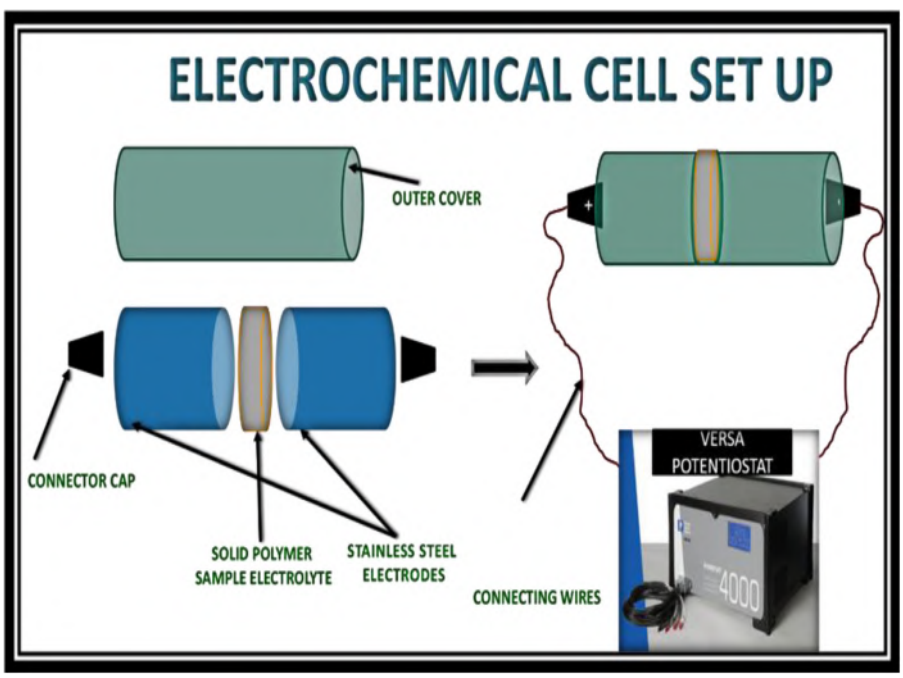

Scheme 2. Schematics for electrochemical set up.

Table 1
Composition data.

EXPT NO	PVDF	Additive	Solvent
1	4.42 g	–	30.66 g NMP
2	2 g	0.1 g CNT	15.5 g NMP
3	2 g	0.2 g CNT	16.05 g NMP
4	2 g	0.3 g CNT	20.54 g NMP
5	2 g	0.4 g CNT	15.23 g NMP
6	2 g	0.5 g CNT	21.29 g NMP
7	1 g	0.1 g CNT fn COOH	6.12 g NMP
8	1 g	0.1 g CNT fn SO_3H	6.18 g NMP
9	1 g	0.15 g CNT fn COOH	6.56 g NMP
10	1 g	0.15 g CNT fn SO_3H	6.67 g NMP
11	1 g	–	7.64 g Acetone
12	1 g	0.1 g CNT	8.36 g Acetone

materials were characterized using XRD, EDS, FE-SEM, Raman, FT-IR and Thermal analysis (TGA-DTA) techniques as discussed below. The synthesized PVDF/CNT composite material and the application in actuation or sensing are shown in Scheme 3.

3. Results and discussion

3.1. X-ray diffraction (XRD) study

The prepared PVDF/CNT composite and functionalized CNT composites are characterized using XRD, EDS, FE-SEM, Raman, FT-IR and Thermal analysis (TGA-DTA) techniques. The details of the results obtained from each analysis are presented one by one below. Fig. 1 shows the XRD pattern of the four different sam-

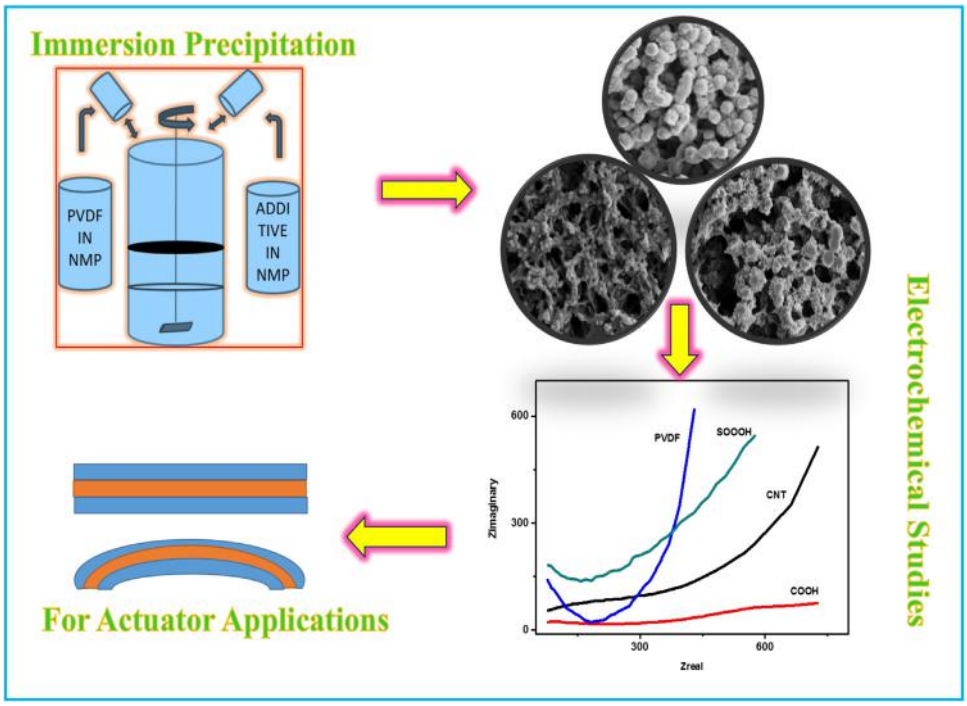

Scheme 3. The synthesized PVDF/CNT composite material and their analysis for application in actuation or sensing are shown in Scheme 3.

ples of PVDF and their composites prepared using the procedure as described above. Spectra A, B, C, and D are the XRD patterns for PVDF, PVDF + CNT, PVDF + CNT with COOH functionalization and PVDF + CNT with SO_3H functionalization samples respectively. The XRD peaks are plotted in the 2θ range of 10–90°. The diffraction patterns shows characteristic peaks originating from different lattice planes for four different samples. From the integration of the area under the crystalline peaks, it can be seen that the pure PVDF membrane (spectra A) contains predominantly major crystalline peaks at the 2θ values of 18.9, 20.47, 36.65 and 39.42° respectively. These peaks are attributed to the crystal planes associated with α, γ, β and α- phases of PVDF respectively. Going by literature, addition of multi walled CNT's promotes the crystallization of the PVDF in the β-polymorph [25]. This is indicated from the XRD patterns of MWCNT-PVDF nanocomposite membranes (spectra B) which exhibit the distinct feature of containing a couple of peaks at 36.46° and 56° which are attributed specifically to the presence of the 101 and 221 planes of β polymorph of PVDF. In addition to this peak, the CNT-PVDF nanocomposite samples also exhibit large reductions in the areas under the peaks associated with other polymorphs that occur at the 2θ values of 20.2° and 39° corresponding to 110 plane of γ and 002 plane of α polymorph respectively. Further peaks at 26.6 and 42.9° are due to CNT only. All peaks are slightly shifted to left. In case of carbonic acid functionalised CNT (spectra C), we have observed similar result with a new peak at 18.43° which is due to presence of COOH functionalised group. But surprisingly, sulphonic acid functionalised CNT (spectra D) mixed PVDF has an XRD pattern akin to that of PVDF with slightly less intense CNT peak at 26.4°. All these XRD peaks of PVDF and CNT match thoroughly with standard JCPDS data file numbered 38–1638 and 75–1621 for PVDF and MWCNT respectively. Similar types of XRD pattern for PVDF and CNT was reported by Mago et al. for their study on membranes of PVDF nano-composites with carbon nanotubes via immersion precipitation [25].

3.2. Field-emission scanning electron microscopy (FE-SEM) analysis

Fig. 2A–D shows the Field-Emission Scanning Electron Microscopy (FE-SEM) images of the pure PVDF, PVDF-CNT, COOH functionalised PVDF-CNT and SO_3H functionalised PVDF-CNT materials prepared via co-precipitation method as described before. The effect of CNTs on the membrane structure is significant and gives rise to the decrease in crystal size and to an increase of the microporosity of the PVDF membranes. From the first micrograph (Fig. 2A), one can perceive an extended sponge-like membranous structure for the pure PVDF membrane in NMP base. This is similar to the one observed by Mago et al. [25]. It resembles a pristine skin embedded with spherulitic crystallites in the 0.8 to 1 μm diameter range. In contrast to this, the second micrograph (Fig. 2B) depicts the effect of incorporation of the CNTs on the distributions of crystallite shapes, sizes, porosity, etc. A detailed morphological study reveals that the spherulites size has reduced remarkably as compared to that of pristine PVDF and they are crystallized on the nanotube surface itself. This may be due to the CNTs acting as heterogeneous nucleating agents, the concentration of which determines the number of nuclei. We conclude that upon the incorporation of the CNTs, a porous framework comprising shish-kebab-like crystalline entities are formed which are loosely interconnected, seemingly endless with open network, structure. Based on such a network, one might expect a better mechanical efficiency of the piezo films. Moreover, the enhancement of directionality of these spherical crystallites can be due to the induced β phase as we had inferred from our XRD data. The enhanced microporous structure becomes more pronounced with a beautifully inter-connected network in case of COOH functionalised PVDF-CNT membrane (Fig. 2C) which corresponds to our XRD results. The approximate size of the particles are ~800 nm range for PVDF, 200 nm range for PVDF-CNT membrane and in 150 nm range for COOH functionalised PVDF-CNT membrane. Finally, the SO_3H functionalised PVDF-CNT membrane (Fig. 2D) shows a flat non-porous 'skin' image without any microstructure. These dense

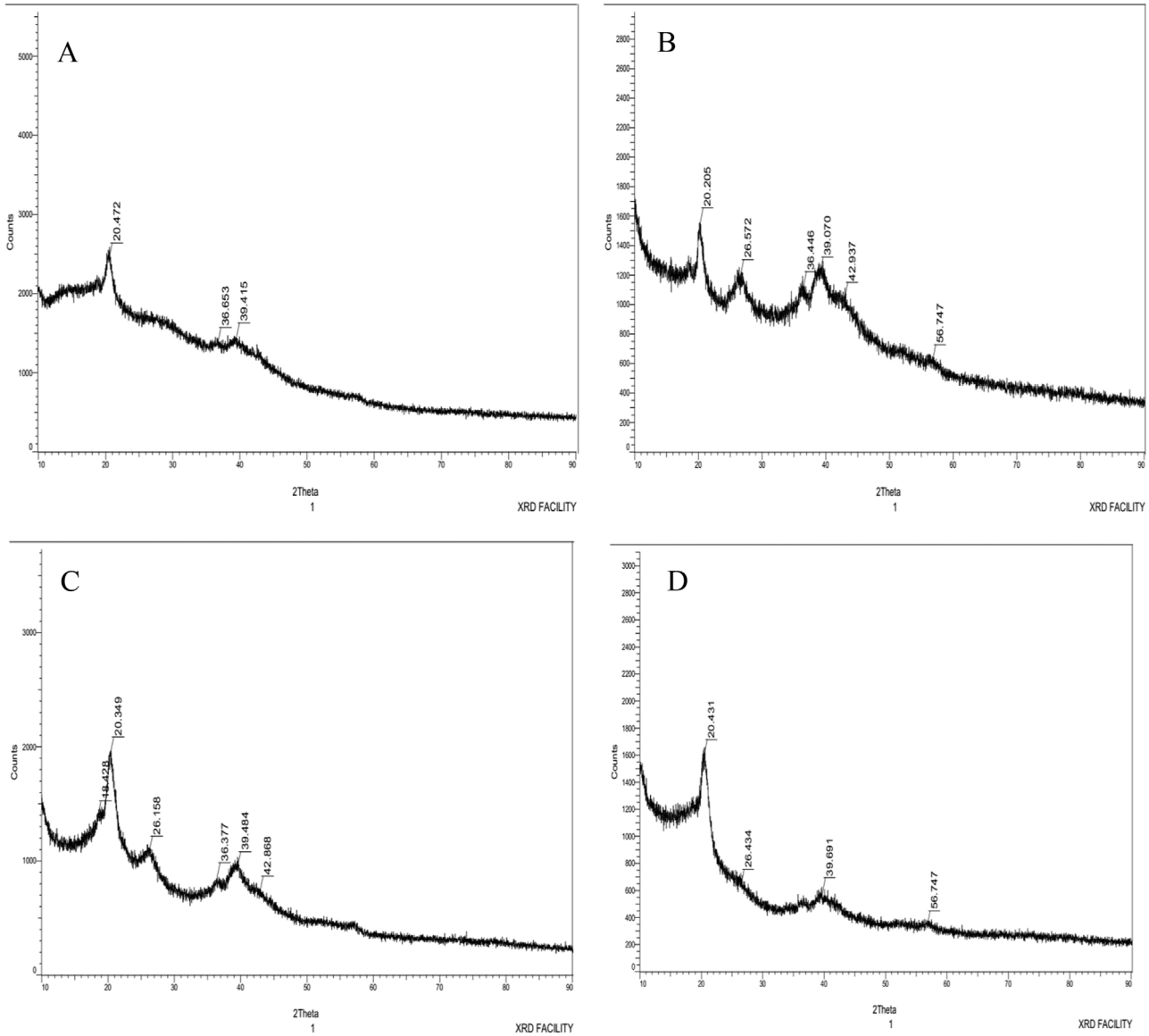

Fig. 1. (A–D): XRD spectra of (A) PVDF, (B) PVDF with CNT, (C) PVDF with carbonic acid functionalised CNT and (D) PVDF with sulphonic acid functionalised CNT.

layered structures can be found in some high density polymers. We presume that this structure may owe its morphology to the incomplete transition due to sulphur doping under given conditions. Fig. 3(A–D) gives the corresponding high magnification FESEM micrographs of the same samples as described above. Besides, it is well known that an increase in porosity leads to a decrease in the transverse piezoelectric coefficient relative to the longitudinal one. This enhances the strain coefficient that is directly proportional to higher electric charges.

3.3. Energy dispersive X-ray spectroscopy (EDS) analysis

Fig. 4 depicts the results obtained from energy dispersive X-ray spectroscopy (EDS) analysis. An EDS analysis is used to determine the elements present in the reaction product. There are four different EDS spectra, amongst which spectra A is for only PVDF, spectra B is for PVDF + CNT, spectra C is for PVDF + CNT with COOH functionalization and spectra D is for PVDF + CNT with SO_3H functionalization samples respectively. All the expected peaks of C, O and F came for spectra A, B and C respectively where spectra D contains additional S peak also due to functionalization of SO_3H group. In our synthesis, we used NMP as solvent which leads to high oxygen content. We have neglected nitrogen content here in order to compare other elements. We can see high carbon and fluorine content is due to PVDF matrix and CNT composite. We have also given the information regarding the amount of solvent used which affects the oxygen content and cannot show the difference in oxygen content due to addition of carbonic and sulphonic acid groups. Interestingly, the low sulphur content in spectra D supports the sulphur doping under given conditions.

3.4. Fourier transform infrared spectroscopy (FT-IR) analysis

Fourier Transform Infrared Spectroscopy (FT-IR) has been used to identify the different functionalities present in our synthesized materials surface. In our study, we used PVDF, CNT and functionalized CNT with COOH and SO_3H group. So a systematic and comparable study will tell us the specific binding of the functional group with the PVDF/CNT surface. A systematic and careful comparison between these four spectra should not only indicate the presence of COOH and SO_3H group on the surface but will help to identify the nature of the interaction taking place among them.

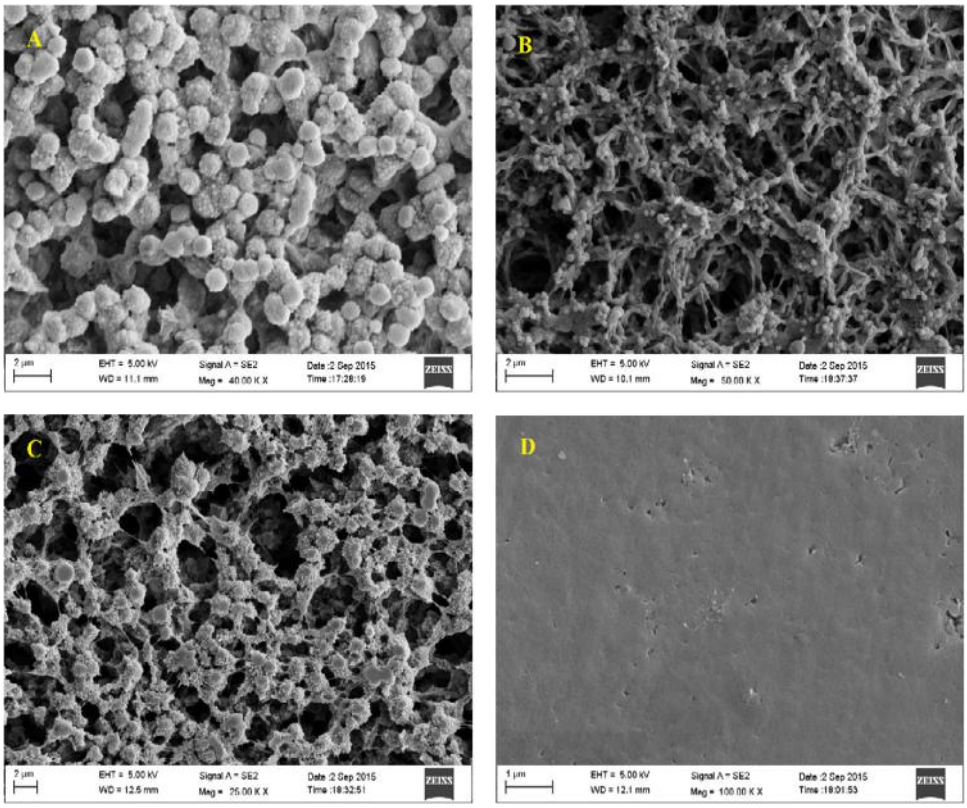

Fig. 2. (A–D): FESEM image of (A) PVDF, (B) PVDF with CNT, (C) PVDF with carbonic acid functionalised CNT and (D) PVDF with sulphonic acid functionalised CNT.

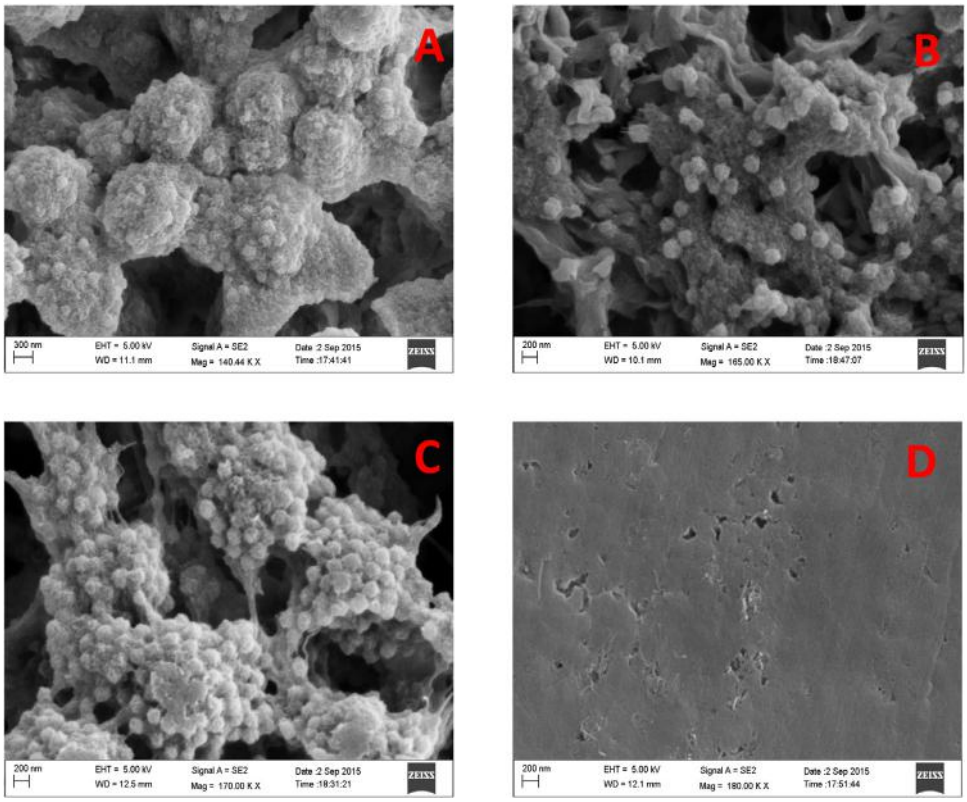

Fig. 3. (A–D) High Magnification FESEM image of (A) PVDF, (B) PVDF with CNT, (C) PVDF with carbonic acid functionalised CNT and (D) PVDF with sulphonic acid functionalised CNT.

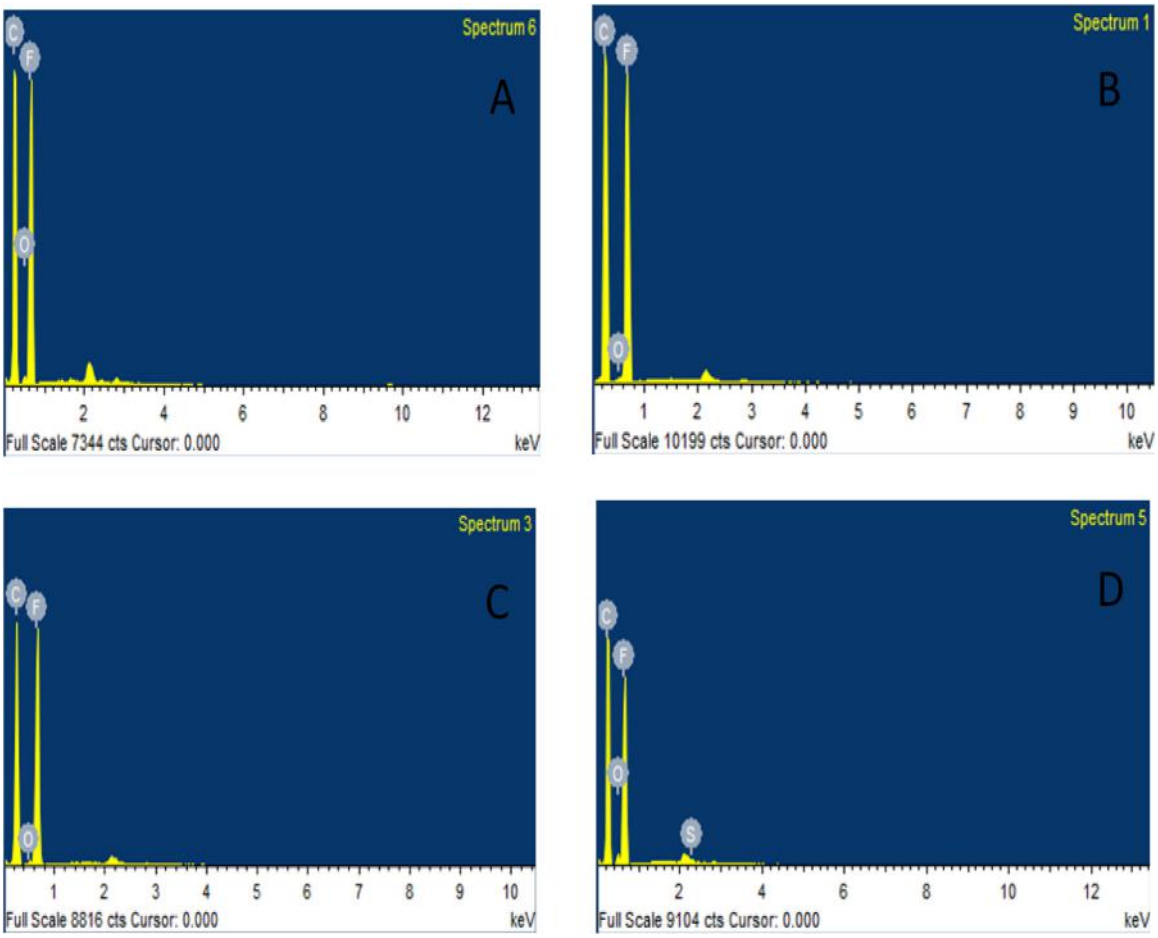

Fig. 4. (A–D) EDAX spectra of (A) PVDF, (B) PVDF with CNT, (C) PVDF with carbonic acid functionalised CNT and (D) PVDF with sulphonic acid functionalised CNT.

Fig. 5, shows the combined FT-IR spectra where curve A indicate for only PVDF, curve B for PVDF + CNT, curve C and D for PVDF with carbonic acid and sulphonic acid functionalised CNT respectively. The entire FT-IR spectra was analysed in the wavenumber region 4000–400 cm^{-1} and the corresponding FT-IR bands are tabulated in Table 2. A broad and distinct peak at 3425, 3408, 3404 and 3394 cm^{-1} for all four sample is observed due to stretching vibration of O—H group. The C—F stretching vibration for PVDF is observed at 872, 874, 876 & 872 cm^{-1} for all four samples and similarly peak in the range of 836–838 cm^{-1} may also depict the β-phase CH_2 rocking peak for PVDF. For carbonic acid functionalised CNT sample, the characteristic C=O stretching, C—O stretching and C—C bending vibration due to carbonic acids are present as sharp peak in 1657 cm^{-1}, low intense peaks in 1064 cm^{-1} and 612 cm^{-1} respectively. Similarly, there is a weak but characteristic C-S stretching peak is present in sulphonic acid functionalised CNT sample (curve D) at 1231 cm^{-1} which is absent in case of other three samples (curve A, curve B and curve C). The peak height for C=O stretching vibration decreases as follows: sulphonic acid functionalised CNT mixed PVDF sample > only PVDF samples >CNT mixed PVDF samples > carbonic acid functionalised CNT mixed PVDF sample. Moreover, the peak shifts from PVDF to CNT to sulphonic acid functionalized CNT to carbonic acid functionalized CNT samples from 1666 to 1657 cm^{-1} indicating the probable interaction and binding on the nanotube surface. The peak between 1232 and 1231 cm^{-1} in bare PVDF and PVDF/CNT is due to CF_2 stretching and it is absent in case of carbonic acid functionalised CNT/PVDF due to strong interaction between CF_2 group of PVDF and carbonyl group of acids. We also observed a low intense peak due to C—N stretching vibration that may probably be due to the NMP used as solvent during synthesis. Anjalin observed similar types of FT-IR spectra for PVDF-MWCNT composites before [26]. Moreover, the strong interaction between the CF_2 group of PVDF and carbonyl group of acids have already shown by Kim et al. [27].

3.5. Thermal analysis

The thermogravimetric analysis (TGA) and differential thermal analysis (DTA) techniques are used to estimate the water of crystallization, decomposition temperatures and finally the stability of the sample for a specific temperature range. The as-prepared samples were heated from RT to 1000 °C with an increment of 10 °C min^{-1} in air. Fig. 6A–D shows the TGA and DTG curve for only PVDF (curve 6A), PVDF + CNT mixture (curve 6B), PVDF + CNT functionalized with COOH (curve 6C) and PVDF + CNT functionalized with SO_3H (curve 6D) respectively. DTG curves are plotted in dotted lines. From the TGA curve of only PVDF (Fig. 6A), a weight loss of about 75% at 150 °C and a further weight loss of about 95% at 500 °C was observed. DTG curve (Fig. 6A) shows three exothermic peaks at 77, 134 and 482 °C with derivative losses corresponding to 0.75, 0.85 and 0.58 respectively. The first two peaks may signify loss of NMP and hydrogen fluoride and second to that of decomposition or carbonisation of PVDF sample. Tar and simple gases, such as hydrogen and methane are evolved and the carbon that remains loses very little mass between 500 °C and 900 °C. In this second stage, the higher the fluorine content of the polymer, the lower the yield of tar. This is because fluorine is able to remove hydrogen, which would otherwise be used in the compounds that form

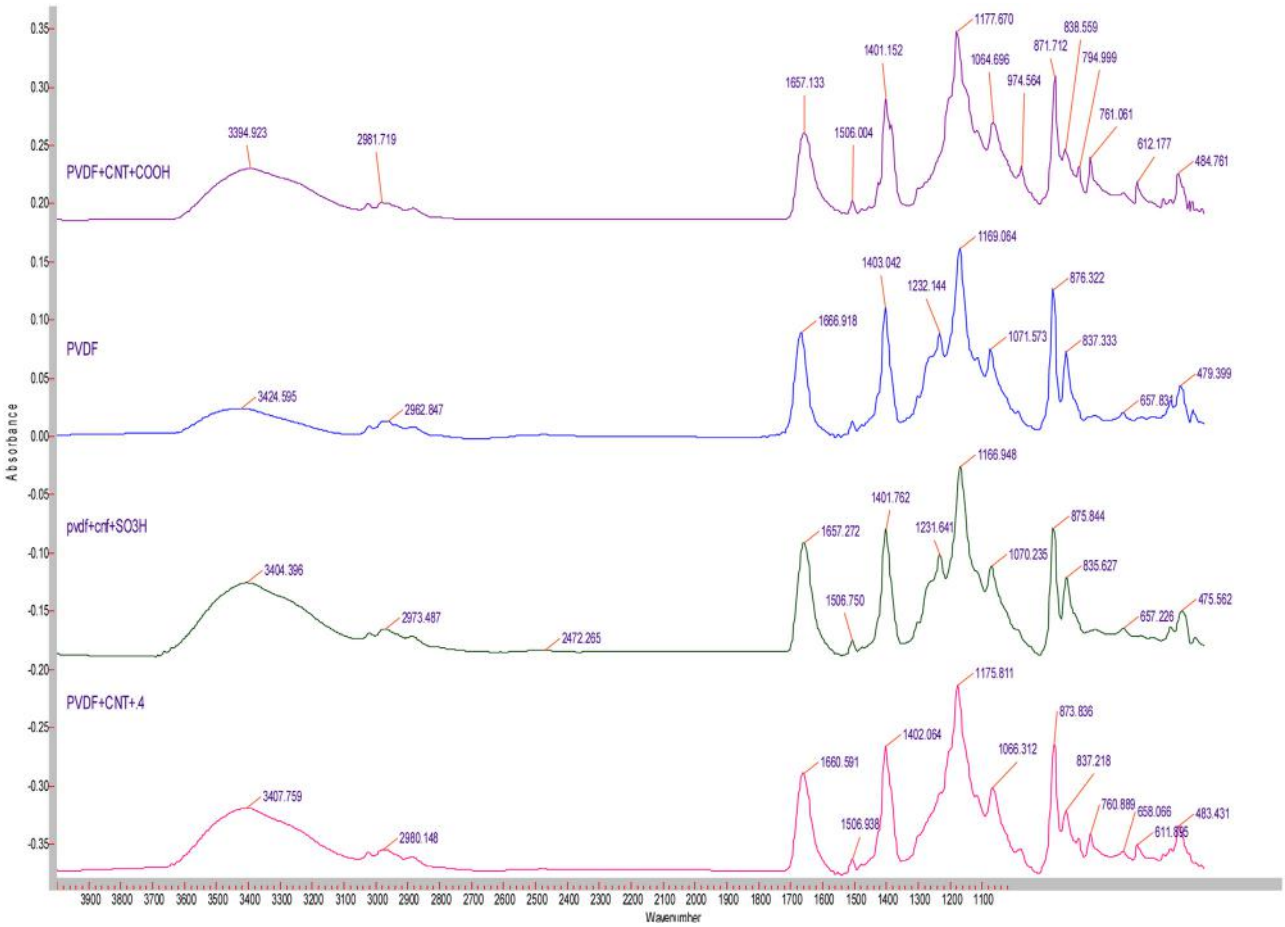

Fig. 5. FT-IR spectra of (A) PVDF, (B) PVDF with CNT, (C) PVDF with carbonic acid functionalised CNT and (D) PVDF with sulphonic acid functionalised CNT.

tar. For PVDF + CNT sample, from the TGA curve (Fig. 6B), there is a weight loss of about 50% at 160 °C and a further weight loss of about 83% at 500 °C was observed. The weight loss at 160 °C is due to loss of moisture or water molecule from the sample. From DTG curve (Fig. 6B), there are two exothermic peaks at 119 and 486 °C with derivative losses corresponding to 0.6 and 0.75 respectively. The first exotherm correspond to loss of HF and second one for the decomposition of PVDF + CNT sample. For PVDF + CNT functionalized with COOH, we find a loss in weight of about 50% at 160 °C and a further loss ~89% at 500 °C as observed from TGA curve (Fig. 6C). The DTG curve (Fig. 6C) shows two exotherm at 117 and 488 °C with derivative losses corresponding to 0.6 and 1.1 respectively. The first loss may correspond to loss of HF and second loss may be decomposition of PVDF + CNT functionalized with COOH sample. Similarly, for PVDF + CNT functionalized with SO_3H, we find a loss in weight of about ~90% at 491.27 °C as observed from TGA curve (Fig. 6D). From DTG curve (Fig. 6D), it shows an exotherm at 491 °C with derivative losses corresponding to 2.3. The loss may correspond to decomposition of PVDF + CNT functionalized with SO_3H sample.

A distinct endo-thermal peak can be seen at 84.15, 65 and 67.09 °C for PVDF, PVDF + CNT and PVDF + CNT functionalized with COOH sample respectively from the respective DTA curves (Fig. 7 A–C). The temperature difference decreases from only PVDF sample to PVDF + CNT sample which might correspond to phase change in the sample. Moreover, it is already reported that the α-β transition occurs at lower temperature on adding CNT. But this peak disappears in PVDF + CNT functionalised with SO_3H sample (Fig. 7D) which may be due to the sulphur at the surface preventing the phase transition. Corresponding to PVDF decomposition, we see small exothermic peaks in DTA curve around 480–500 °C. But the peak shows sudden spike for SO_3H functionalised samples which may be due to the fact that sulphur decomposition too occurs at around the same temperature range. A similar type of TGA-DTA curve for PVDF and PVDF with CNT was observed before by others [28].

3.6. *Electrochemical analysis of PVDF/CNT and their functionalized composites for applications in actuation and sensing*

3.6.1. *Cyclic voltametric (CV) study*

Fig. 8 shows the Cyclic Voltametric (CV) study of the synthesized PVDF, CNT and their functionalized materials. The potential window we used in our present study is from 0 to 1 V based on our needs. From Fig. 8, we can see that as we move from PVDF to PVDF + CNT functionalized with SO_3H sample, we observe the following trend. The maximum current increases from PVDF to PVDF + CNT functionalized with COOH sample but it is almost equal in case of PVDF + CNT functionalized with SO_3H sample. The maximum current values are as follows: 0.0085 mA for only PVDF, 0.34 mA for PVDF + CNT, 2.7 mA for PVDF + CNT functionalized with COOH and 0.14 mA for PVDF + CNT functionalized with SO_3H group respectively. So by analyzing the datas we can see that the observed maximum current values for PVDF + CNT functionalized with SO_3H sample is higher than that of pure PVDF but it is much lower than other two sample such as PVDF + CNT and PVDF + CNT functionalized with COOH group. Moreover, not surprisingly, the PVDF and

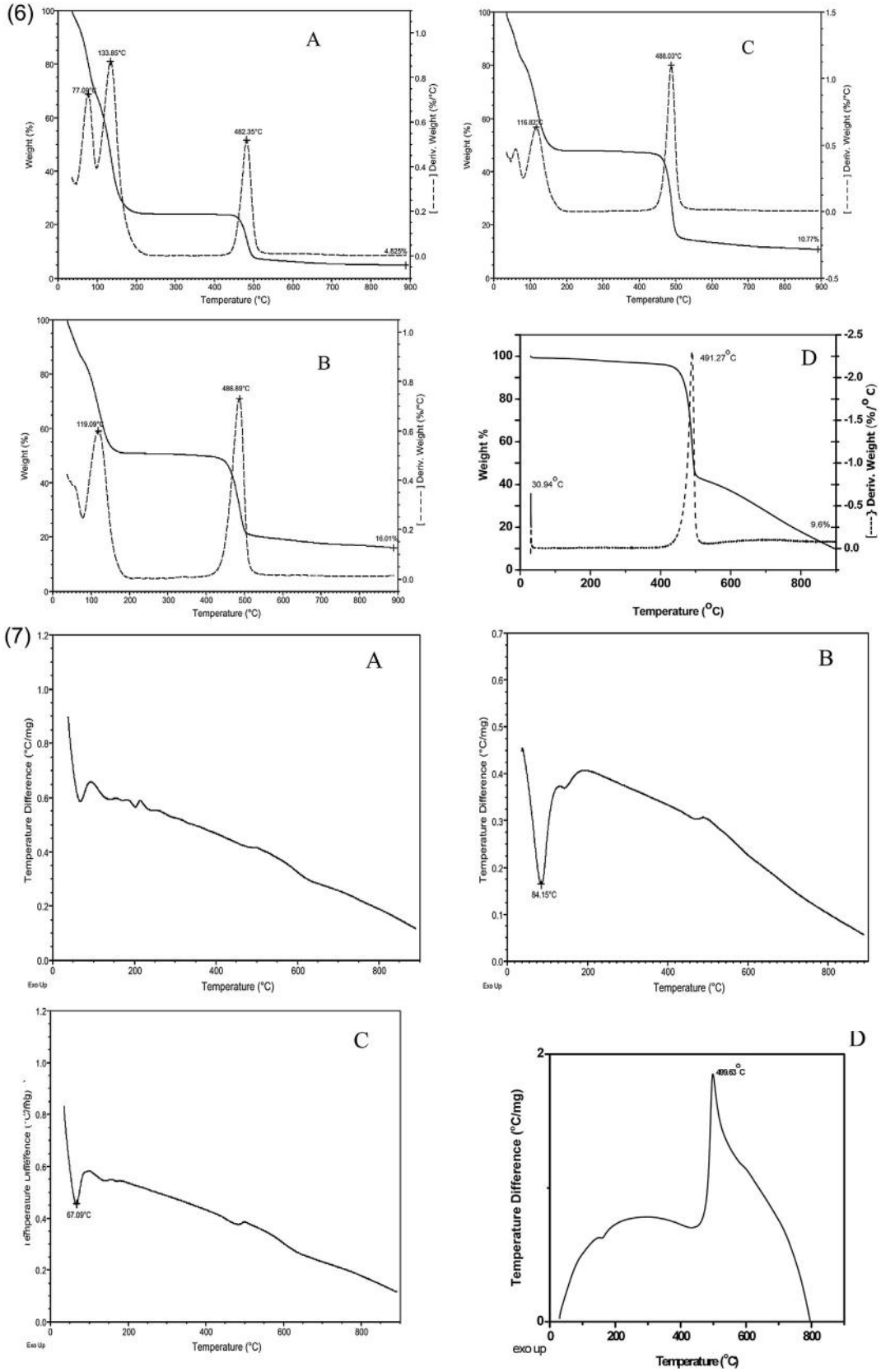

Figs. 6–7. (A–D) TGA-DTA curve of (A) PVDF, (B) PVDF with CNT, (C) PVDF with carbonic acid functionalised CNT and (D) PVDF with sulphonic acid functionalised CNT.

PVDF + CNT functionalized with SO_3H group have similar difference between the reduction and oxidation curves while the other two curves have higher differences but their oxidation and reduction curves are overlapping each other. Besides, we don't find any strong oxidation or reduction peak in any of these cases indicating the electrical stability of the polymer matrix.

Table 2
FT-IR peak analysis data.

PVDF		
Wave number	Absorbance	Functional group
3424.595(b)	0.027	O—H stretch
2962.849(s)	0.019	C—H stretch
1666.918(sh)	0.088	C=O stretch
1403.402(m)	0.107	C—C stretch
1071.573(s)	0.067	C—O stretch
871.712(m)	0.12	C—F stretch
837.333(s,b)	0.063	N—H wag
1169.069(m)	0.158	C—N stretch
PVDF + CNT		
Wave number	Absorbance	Functional group
3407.759(b)	0.05	O—H stretch
2980.148(s)	0.019	C—H stretch
1660.591(sh)	0.081	C=O stretch
1402.264(m)	0.106	C—C stretch
1070.235(s)	0.065	C—O stretch
873.836(m)	0.112	C—F stretch
837.218(s,b)	0.054	N—H wag
1175.811(m)	0.159	C—N stretch
760.889(s)	0.046	C—C Aliphatic vibration
611.895(s)	0.026	C—H bend
PVDF + COOH fn CNT		
Wave number	Absorbance	Functional group
3394.923(b)	0.047	O—H stretch
2981.719(s)	0.019	C—H stretch
1657.133(sh)	0.07	C=O stretch
1401.152(m)	0.1	C—C stretch
1064.696(s)	0.077	C—O stretch
871.712(m)	0.12	C—F stretch
838.559(s,b)	0.052	N—H wag
1177.67(m)	0.16	C—N stretch
764.999(s)	0.046	C—C Aliphatic vibration
612.177(s)	0.029	C—H bend
PVDF + SO_3H fn CNT		
Wave number	Absorbance	Functional group
3404.396(b)	0.05	O—H stretch
2973.487(s)	0.02	C—H stretch
1657.272(sh)	0.093	C=O stretch
1401.762(m)	0.102	C—C stretch
1070.235(s)	0.065	C—O stretch
875.847(m)	0.107	C—F stretch
835.627(s,b)	0.058	N—H wag
1166.948(m)	0.156	C—N stretch
1231.641	0.078	C—S stretch

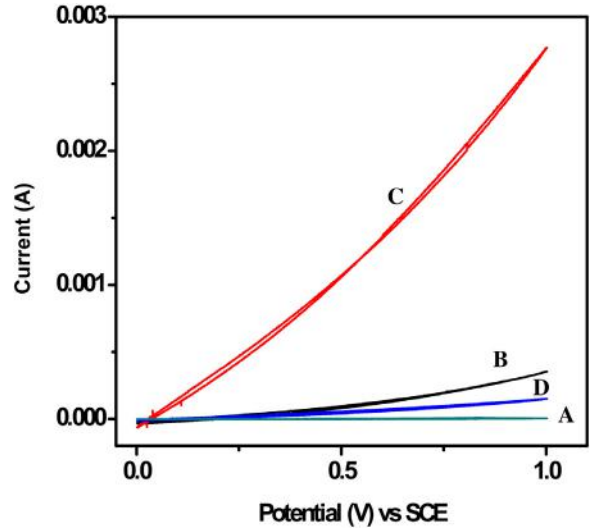

Fig. 8. (A–D) Cyclic voltammogram of (A) PVDF, (B) PVDF with CNT, (C) PVDF with carbonic acid functionalised CNT and (D) PVDF with sulphonic acid functionalised CNT.

3.6.2. Impedence studies

The electrochemical impedance studies are done by analysing three plots such as Nyquist or Cole-Cole plot, Bode frequency plot and Bode phase angle plot using you fabricated materials. Nyquist plot deals with −ve imaginary part of impedance versus the real part of impedance. Bode frequency plot involves magnitude of impedance versus frequency and Bode phase angle plot considers magnitude of impedance versus phase angle. Here, we take into account the most commonly used Nyquist plot for our study. In this plot, at higher frequency, we observe semi-circle with peak denoting capacitive reactance (Xc) that can be co-related to capacitance as $Xc = 1/\omega C$ and where $\omega = 2\pi F$. Moreover, the diameter denotes polarisation resistance and at lower frequency, we obtain a linear curve with slope proportional to Warburg resistance [29]. In this case, the high frequency arc can be represented by a parallel combination of a constant phase element (due to the immobile polymer chains that became polarized in an alternating field) and a resistor (due to the mobile ion in the polymer matrix). The low frequency spike is attributed to the double layer response at the electrode electrolyte interface.

Fig. 9 shows the Nyquist plot using our four different samples. From the plot we can see that as we move from PVDF to PVDF + CNT functionalized with SO_3H group, the capacitive reactance and polarisation resistance values are decreasing till PVDF + CNT functionalized with COOH group and are seemingly equal with that of PVDF + CNT functionalized with SO_3H group. They values are approximately 600, 300, 100 and 600 Ω respectively in terms of polarisation resistance. The capacitive reactance is proportional to Y-Axes value (corresponding to the highest point loci of the dome shaped part of the Nyquist plot) that goes as 160, 90, 30 and 190 respectively. But on the other hand the slope of the linear part denoting Warburg resistance is decreasing from PVDF to PVDF + CNT functionalized with SO_3H group. The slopes can be taken on an average as 1.9, 0.9, 0.7 and 0.6. (here one must recall that a slope of 1 denotes diffusion governed process while slope of ∞ depicts purely capacitive process). Using ZSimpWin (by iteration to get minimum error), we had found that for PVDF and PVDF + CNT functionalised with SO_3H, circuits maybe LR(QR) or R(C(RW)); for PVDF + CNT, maybe (C(R(LR))) or (C(RW)) and for PVDF + CNT functionalised with COOH, circuits maybe (CR(LR)) or (C(RW)). So we conclude that on adding COOH functionalization to PVDF + CNT, we are improving the electro-resistive behaviour but decreasing the capacitance. Now, while adding SO_3H functionalised CNT, we make it comparable to that of pure PVDF [30]. By using the formula, $\sigma = l/R_bA$, we can plot the conductivity versus frequency curve which shall follow the same trend as that of saturated current in the CV data. The thickness 'l' and area 'A' remain constant for all impedance readings and the conductivity being inverse of polarisation resistance, so it become maximum for COOH functionalized CNT + PVDF. Moreover, as discussed in the introduction part, it is the electrical property of MWCNT that plays key role in nanocomposites for pneumatic and other actuators and piezoelectric sensors. The actuators combine piezo-active property of PVDF and piezo-resistive property of CNTs. Here, based on electrochemical studies, we have shown that the carbonic acid functionalised CNT based PVDF composites have shown better electrical property than only CNT based PVDF composites which makes them more suitable nanofillers. But, at this point, same can't be said for SO_3H functionalized CNT + PVDF.

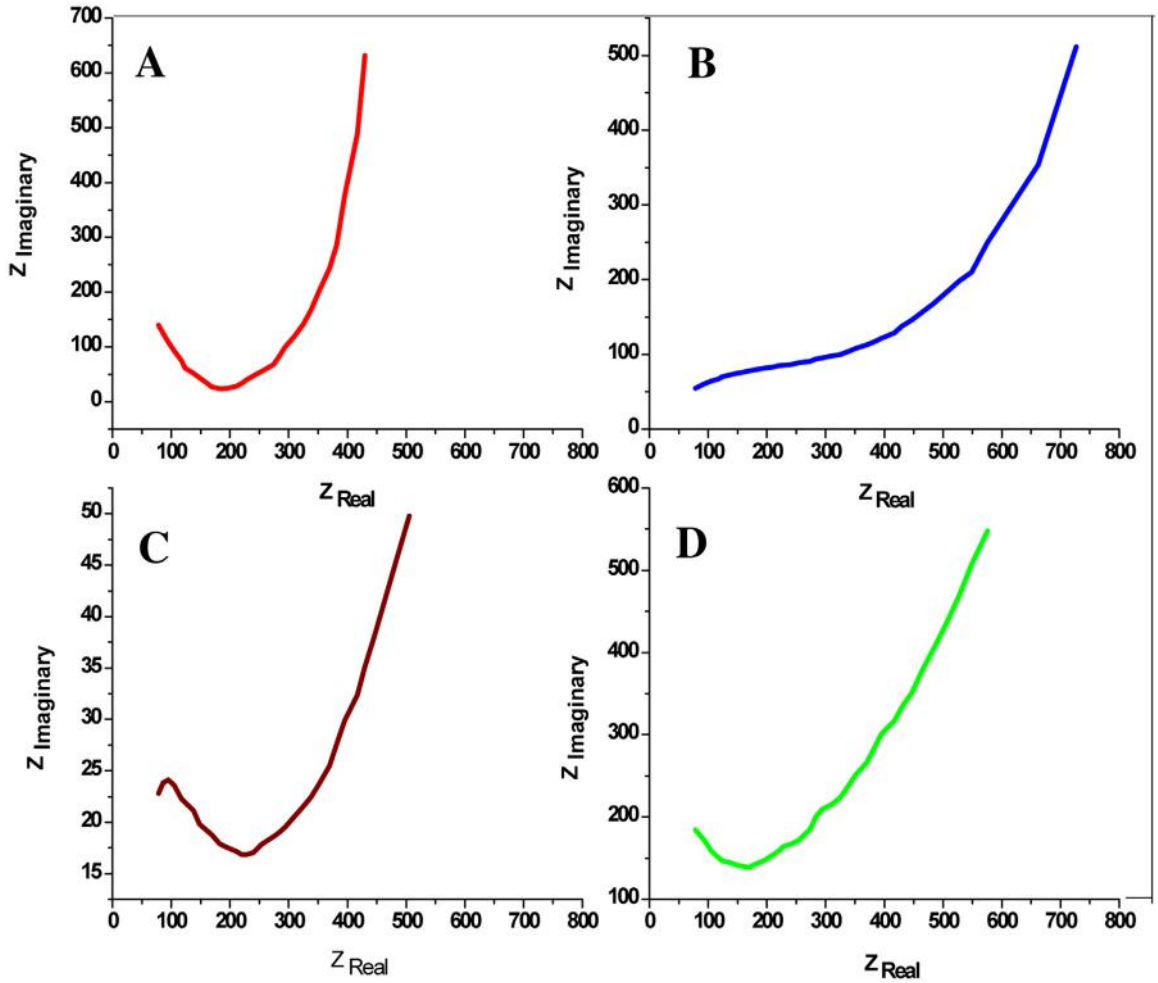

Fig. 9. (A–D) Electrochemical Impedance spectra of (A) PVDF, (B) PVDF with CNT, (C) PVDF with carbonic acid functionalised CNT and (D) PVDF with sulphonic acid functionalised CNT.

4. Conclusion

In conclusion, we have successfully prepared PVDF piezoelectric films with *N*-Methyl-2-pyrrolidone and have modified the films with piezo resistive carbon nano tubes (CNT) and carbonic and sulphonic acid functionalised CNTs. We observed that at a certain concentration of PVDF and CNT, they formed well crystalline morphology with specific structures. After optimizing their concentrations, we functionalized CNT with carbonic and sulphonic acid groups by adding suitable functionalizing agents. The synthesized composite materials were characterized by different spectroscopic and microscopic techniques. From FE-SEM analysis, the sheikh kabab morphology was observed in PVDF while more pronounced and oriented structure was found in case of CNT as well as their functionalized product. The synthesized materials are studied for actuation and sensing purposes by investigating their properties using electrochemical studies such as cyclic voltammetry (CV) and electrochemical impedance spectroscopy (EIS) analysis. It was observed that the actuation properties of PVDF was enhanced while mixed with CNT and carbonic acid functionalized CNT although it remained unchanged in case of sulfonic acid functionalized CNT. In case of PVDF and carbonic acid functionalized CNT, a higher saturation current of 2.7 mA was observed while for bare PVDF in NMP, a reduced value of 0.0087 mA was observed. Similarly, the polarisation resistance was minimum for carbonic acid functionalized CNT, slightly higher for CNTs and almost comparable for bare PVDF and sulfonic acid functionalized CNT/PVDF composites. Hence, by electrochemical studies we prove that carbonic acid functionalised CNTs nanofiller based PVDF films might have embarked upon an improvement over traditional PVDF films for actuation or sensing based applications while sulphonic acid functionalized CNTs are not better nanofillers under similar preparatory conditions. This might be due to the strong interaction between CF_2 group of PVDF and carbonyl group of carbonic acid. The present synthesis route and their application process is simple, less time consuming and could be further extended in near future for the fabrication of other composite materials for their potential application in different energy related fields and various other electromechanical studies like electrical percolation threshold, piezoelectric strain constant, piezoelectric voltage constant, electromechanical coupling factor [31], piezoelectric and viscoelastic moduli [32], piezoelectric resonance and efficiency purposes to prove our hypothesis.

Acknowledgements

We are deeply indebted to our venerated Director of CECRI, Dr. V. K. Pillai and our dean Dr. B. Ramesh Babu for granting us permission to carry out our project work in ISRO-IISU. We can hardly express our heartfelt obligations to VSSC, ISRO for helping us with our preliminary characterisation studies and we are even more obliged to Dr. Sathish in VSSC for helping us in hot-pressing of our samples. We are also gratified that PPEG, IISU allowed us to carry out our project in IISU for a period of three months.

References

[1] B. Mika, Design and testing of piezoelectric sensors, in: PhD Thesis, Texas A&M Univ., 2009, pp. 109.
[2] M. Marutake, The days when piezoelectric PVDF was discovered, Ferroelectrics 2014 (1995) 5–6.
[3] A. Lüker, A short history of ferroelectricity, Ther. Ggw. 115 (10) (1976) 1796–1802.
[4] P. Taylor, T. Furukawa, Phase transitions: a multinational ferroelectric properties of vinylidene fluoride copolymers, Phase Trans. 18 (1989) (1989) 143–211.
[5] S. Anjana Jain, P.N. Rashmi, S.Jayanths Kumar, J.C. Dielectric, Behaviour of PVDF thin films, Indian J. Adv. Chem. Sci. 2 (3) (2014) 28–35.
[6] T. Furukawa, Piezoelectricity and pyroelectricity in polymers, IEEE Trans. Electr. Insul. 24 (3) (1989) 375–394.
[7] D. Esterly, Manufacturing of poly (vinylidene fluoride) and evaluation of its mechanical properties, in: MSc Thesis, Virginia Polytech. Inst., 2002, pp. 1–66.
[8] S.A. Carabineiro, M.F. Pereira, J.N. Pereira, C. Caparros, V. Sencadas, S. Lanceros-Mendez, Effect of the carbon nanotube surface characteristics on the conductivity and dielectric constant of carbon nanotube/poly(vinylidene fluoride) composites, Nanoscale Res. Lett. 6 (1) (2011) 302.
[9] a. Ferrreira, J.G. Rocha, a. Ansón-Casaos, M.T. Martínez, F. Vaz, S. Lanceros-Mendez, Electromechanical performance of poly(vinylidene fluoride)/carbon nanotube composites for strain sensor applications, Sens. Actuators A Phys. 178 (2012) 10–16.
[10] V. Choudhary, A. Gupta, Polymer/carbon nanotube nanocomposites, Intech (2001) 65–90.
[11] B. Pinto, S. Kern, J.J. Ku-Herrera, J. Yasui, V. La Saponara, K.J. Loh, A comparative study of a self strain-monitoring carbon nanotube film and carbon fibers under flexural loading by electrical resistance changes, J. Phys. Conf. Ser. 628 (2015) 012098.
[12] M. Njuguna, Characterisation of multi wall carbon nanotube–polymer composites for strain sensing applications, in: PhD Thesis, Queensl. Univ., 2012, pp. 210.
[13] C.-X. Liu, J.-W. Choi, Improved dispersion of carbon nanotubes in polymers at high concentrations, Nanomaterials 2 (4) (2012) 329–347.
[14] A.L.V.G. O'Bryan, E.L. Yang, T. Zifer, K. Wally, J.L. Skinner, Nanotube surface functionalization effects in blended multiwalled carbon nanotube/PVDF composites, J. Appl. Polym. Sci. 120 (2011) 1379–1384.
[15] Y. Sun, H. Da Bao, Z.X. Guo, J. Yu, Modeling of the electrical percolation of mixed carbon fillers in polymer-based composites, Macromolecules 42 (1) (2009) 459–463.
[16] Z. Spitalsky, G. Tsoukleri, D. Tasis, C. Krontiras, S.N. Georga, C. Galiotis, High volume fraction carbon nanotube-epoxy composites, Nanotechnology 20 (40) (2009) 405702.
[17] Y.C. Jung, H.H. Kim, Y.A. Kim, J.H. Kim, J.W. Cho, M. Endo, M.S. Dresselhaus, Optically active multi-walled carbon nanotubes for transparent, conductive memory-shape polyurethane film, Macromolecules 43 (14) (2010) 6106–6112.
[18] S. Yu, W. Zheng, W. Yu, Y. Zhang, Q. Jiang, Z. Zhao, Formation mechanism ofβ-phase in PVDF/CNT composite prepared by the sonication method, Macromolecules 42 (22) (2009) 8870–8874.
[19] C.-Y. Li, T.-W. Chou, Strain and pressure sensing using single-walled carbon nanotubes, Nanotechnology 15 (11) (2004) 1493–1496.
[20] S. Paulson, M.R. Falvo, N. Snider, A. Helser, T. Hudson, A. Seeger, R.M. Taylor, R. Superfine, S. Washburn, In situ resistance measurements of strained carbon nanotubes, Appl. Phys. Lett. 75 (19) (1999) 2936–2938.
[21] Ö. Pekcan, G.A. Evingür, Conductivity percolation of carbon nanotubes in polyacrylamide gels, Carbon Nanotub. Polym. Nanocomposites (2006) 197–212.
[22] X. Zeng, X. Xu, P.M. Shenai, E. Kovalev, C. Baudot, N. Mathews, Y. Zhao, Characteristics of the electrical percolation in carbon nanotubes/polymer nanocomposites, J. Phys. Chem. C 115 (44) (2011) 21685–21690.
[23] KHY, D.S.B. Sang-Ha Hwang, Young-Bin Park, Smart Materials and Structures Based on Carbon Nanotube Composites, Carbon Nanotub. Synth. Charact. Appl. (2011).
[24] S.K. Tripathi, A. Gupta, M. Kumari, Dielectric and Modulus spectra_studies on electrical conductivity and dielectric behaviour of PVdF–HFP–PMMA–NaI polymer blend electrolyte, Bull. Mater. Sci. 35 (6) (2012) 969–975.
[25] G. Mago, D.M. Kalyon, F.T. Fisher, Membranes of polyvinylidene fluoride and PVDF nanocomposites with carbon nanotubes via immersion precipitation, J. Nanomater. 2008 (2008) 1–8.
[26] F.M. Anjalin, Synthesis and characterization of MWCNTs/PVDF nanocomposite and its electrical studies, Der. Pharma. Chem. 6 (1) (2014) 354–359.
[27] G.H. Kim, S.M. Hong, Y. Seo, Piezoelectric properties of poly (vinylidene fluoride) and carbon nanotube blends: β −phase development, Phys. Chem. Chem. Phys. (2009) 10506–10512.
[28] Varrla Eswaraiah, S.R. Varrla, Eswaraiah Krishnan Balasubramaniam, Afrl-Rx-Wp-Tp-2012-0277 morphological thermal, electrical and electromechanical properties of polyvinylidene fluoride (Pvdf) –, Report IITM (2012) 17.
[29] T. Grygar, F. Marken, U. Schröder, F. Scholz, Electrochemical analysis of solids. a review, Collect. Czechoslov. Chem. Commun. 67 (2) (2002) 163–208.
[30] M.H.P. Tamilselvi, Impedance studies of polymer electrolyte based on PVA, Int. J. Chemtech. Res. 6 (3) (2014) 1864–1866.
[31] K. Uchino, Introduction to piezoelectric actuators and transducers kenji uchino, international center for actuators and transducers, penn state university, Report Int. Cent. Actuators Transducers Penn State Univ. 5 (2003) 40.
[32] L. Seminara, M. Capurro, P. Cirillo, G. Cannata, M. Valle, Electromechanical characterization of piezoelectric PVDF polymer films for tactile sensors in robotics applications, Sens. Actuators A Phys. 169 (1) (2011) 49–58.

View publication stats